

Effect of micro- and macroporosity of bone substitutes on their mechanical properties and cellular response

A. BIGNON¹, J. CHOUTEAU^{2,3}, J. CHEVALIER^{1,*}, G. FANTOZZI¹, J.-P. CARRET^{2,3}, P. CHAVASSIEUX⁴, G. BOIVIN⁴, M. MELIN⁵, D. HARTMANN⁵

¹*Institut National des Sciences appliquées, Groupe d'Etude de Métallurgie Physique et de Physique des Matériaux, CNRS Unité 5510, bat. Blaise Pascal, 20 av. Albert Einstein, 69621 Villeurbanne, France*

*E-mail: jerome.chevalier@insa-lyon.fr

²*Laboratoire MECAL, Faculté de médecine Lyon-Sud, Chemin du petit Revoyet, 69600 Oullins, France*

³*Service de chirurgie orthopédique, Pav. T, Hôpital Edouard Herriot, 5 place d'Arsonval, 69437 Lyon, France*

⁴*INSERM Unité 403, Faculté de Médecine R. Laennec, 8 rue Guillaume Paradin, 69372 Lyon Cedex 08, France*

⁵*Laboratoire des biomatériaux, EA 3090, Faculté de pharmacie, 8 av. Rockefeller 69373 Lyon, France*

The control of porosity morphology and physico-chemical characteristics of calcium phosphate bone substitutes is a key-point to guaranty healing success. In this work, micro- and macroporosity of materials processed with 70% Hydroxyapatite (HAP) and 30% β -tricalcium phosphate (β -TCP) were controlled by sintering temperature and porogen addition, respectively. Porosity was quantified by scanning electron microscopy (pore size) and mercury intrusion porosimetry (interconnection between pores). The content of macrointerconnections and their size were dependent on porogen content, shape, and size. Mechanical properties (compressive strength) were strongly dependent on macroporosity size and content, on the basis of exponential laws, whereas microporosity ratio was less influent. Relying on those results, three types of materials with contrasting porous morphologies were processed and assessed *in vitro*, in primary culture of human osteoblasts and fibroblasts. With both types of cells, an exponential cellular growth was effective. Cells colonized the surface of the materials, bridging macroporosity, before colonizing the depth of the materials. Cell migration across and into macroporosity occurred via the emission by the cells of long cytoplasmic extensions that hanged on microporosity. Both macroporosity and macrointerconnectivity size influenced the penetration of cells. An interconnection size of 15 μm appeared to be effective to support this invasion without bringing down mechanical strength.

© 2003 Kluwer Academic Publishers

1. Introduction

Biphasic calcium phosphate bone substitutes processed from hydroxyapatite (HAP) and β -tricalcium phosphate (β -TCP) are now considered as the most promising alternative to autologous bone grafts [1, 2]. HAP phase, which is very similar to the mineral composition of bone, is highly osteoconductive but is not resorbable. Resorption is necessary for bone to replace progressively the implant and accommodate stress at the interface between the implant and bone. Therefore, β -TCP has been progressively introduced in the composition of bone substitutes because of its dissolution potential [3]. It is

admitted that the rate of resorption *in vivo* is linked to the HAP:TCP ratio of the implanted material [4]. However, differences observed between different commercial biphasic bone substitutes in terms of bone ingrowth are not actually fully explained.

The amount, the size, and the interconnectivity of macropores must have a key influence on bone ingrowth. Interconnections between pores are necessary to promote body fluid circulation and cell migration to the core of the implant. It is generally admitted that a pore size larger than 100 μm is necessary, but the optimum interconnection size is still under debate [5, 6]. Most of the time the

*Author to whom all correspondence should be addressed.

interconnectivity of commercial synthetic bone substitutes is not quantified. High porosity content seems to favor bone ingrowth as the vacant volume of macroporosity can be colonized by bone immediately. Less amount of material has to be resorbed in order to be replaced by the host bone. However, it must be kept in mind that increasing the porosity content and/or size decreases drastically mechanical properties. Calcium phosphate ceramics exhibit weak mechanical strength [7] associated with a high sensitivity to slow crack growth in the presence of water under cyclic stresses [8, 9]. *In vivo* conditions are thus aggressive for those materials: cracks can propagate in the implants and lead to failure. This can be very damaging to the patient, as the implant stability is known to be of main importance for healing success.

Literature is sparse about the influence of microporosity morphology on bone formation [10]. This microporosity is located between ceramic grains when the material is sintered at low temperature. Its morphology can change the properties of the surface of the walls between macroporosities, i.e. the surface directly in contact with bone cells. It can be guessed that changing roughness, specific surface area, and permeability of the walls will affect the affinity of cells with the material. However, the microporosities can again influence the material cohesion as they weaken grain boundaries when their amount increases. Furthermore, they drive physiologic fluids into the core of the material, between grain boundaries, which contributes to weaken them as well and favor the material resorption *in vivo*.

The aim of this study was to process and characterise biphasic bone substitutes with a large range of micro- and macroscale porosities. This porosity was quantified in terms of volume content, size, interconnectivity, and surface properties. The influence of the porosity on the mechanical strength was determined. *In vitro* studies were performed to evaluate the proliferation of fibroblasts and osteoblasts cultured on these bone substitutes. The aim was to give surgeons scientific arguments to choose, for a given clinical indication, the accurate bone substitute in terms of osteoconduction and mechanical strength.

2. Materials and methods

2.1. HAP and TCP powders

High purity grade HAP powder with a Ca/P ratio of 1.67 (Coating Industries, Vaulx-En-Velin, France) and TCP powder with a Ca:P ratio of 1.50 (Merck, Darmstadt, Germany) were used for these investigations. Their initial specific area (determined by 5-points BET method with a Micromeritics ASAP 2010 adsorption analyzer) were 31 and 67 m²/g, respectively.

2.2. Processing

Processing of bone substitutes from HAP and TCP powders was conducted by pressure casting. The method and experimental parameters were detailed in Bignon *et al.* [11]. Slurries were prepared in water with a HAP:TCP weight ratio of 70:30 and an electro-steric dispersant. The dry matter content was fixed to 60%. Ball milling was conducted during 3 h via 2 mm zirconia

beads with a shaker-mixer (Turbulat) to homogenize the slurry. In order to process macroporous architectures, a porogenic agent (polyvinyl butyral) was added before the casting of the slurries. The size of the porogen was either 300–600 or 600–1250 µm and was introduced with ratios ranging from 0 to 65 vol% of the dry matter content. In order to avoid cracking during the thermal degradation of the porogen, a strengthening agent was added in the slurry. The slurries were then casted to obtain green compacts. After debinding at 600 °C to degrade the organic compounds contained in the green ceramics, the materials were naturally sintered in air at temperatures ranging from 1125 to 1250 °C. The macroporosity volume, morphology, and interconnection were controlled by the porogen size, shape, and content whereas the microporosity was controlled by sintering temperature and duration.

2.3. Characterization

Observations of micro- and macropores were conducted with a Jeol 840 ALGS scanning electron microscope (SEM). Interconnection size between micro- and macroporosities and their respective fraction were quantified by mercury intrusion porosimetry with a Micromeritics WIN 9400 apparatus. This method consists in intruding mercury in the porosity of a material, through interconnections, by applying a pressure. For low applied pressures, mercury can only penetrate through large interconnections. On the contrary, high pressures must be applied to penetrate through small interconnections. For each pressure, the intrusion volume is measured. Thus, to a given interconnection size corresponds a volume of porosity that is filled by mercury. By this method, the volume distribution of pores accessible by a given interconnection size can be quantified for a sample of about 1 cm³.

Grain size was measured, according to the linear intercept method [12], from four different SEM micrographs of each material.

Compressive strength was measured with an Instron 8502 on cylindrical machined blocks of 9 mm diameter and 11 mm height. Six samples were used for each measured point.

2.4. Cell culture

Cell cultures were conducted separately on osteoblasts and fibroblasts. Osteoblasts were extracted from cancellous bone of human femoral heads and cultured for 21 days before their seeding on the bioceramics. Fibroblasts were obtained from human skin. Osteoblasts and fibroblasts were then seeded on the surface of biomaterial discs (9 mm diameter and 2 mm thick) and cultured during 4–28 days in 48 wells plates (Falcon, Becton Dickinson Labware Europe, Le Pont De Claix, France).

At day 4, 8, 15, 21 and 28, cell proliferation was evaluated by colorimetric MTT assay [13]. 125 µl of MTT (5 mg/ml of 3-(4, 5-dimethylthiazol-2-yl)-2, 5-diphenyl tetrazolium bromide) Sigma, St Quentin-Fallavier, France) in phosphate-buffered saline were added. After 4 h incubation at 37 °C, the medium was removed and 500 µl of ethanol/DMSO (vol/vol) were

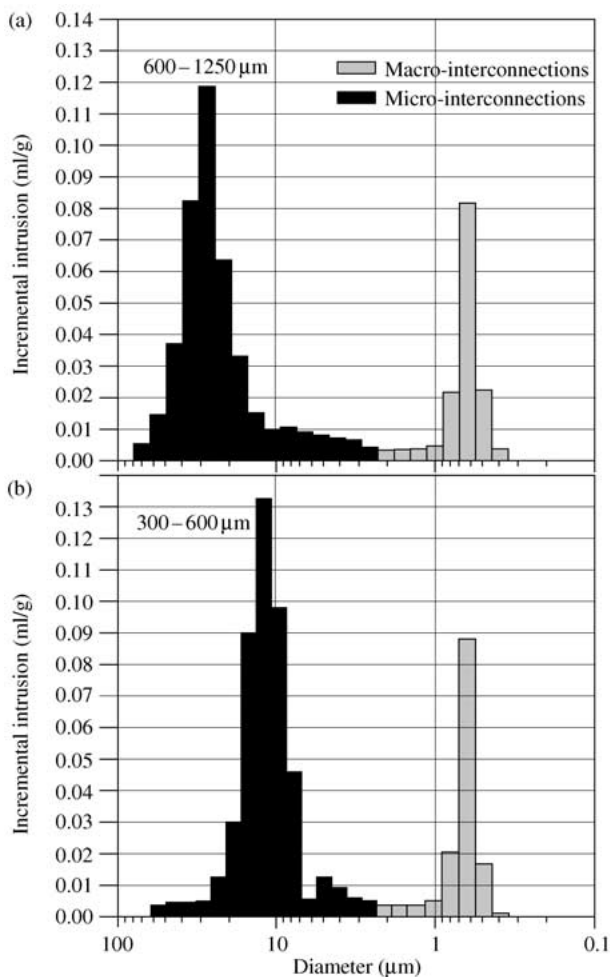


Figure 1 Mercury intrusion diagrams (mercury intrusion volume vs. interconnection diameter) of bone substitutes processed with 65 vol % of 600–1250 μm (a) or 300–600 μm (b) porogen particles. Sintering: 1125 $^{\circ}\text{C}$ during 15 h.

added. After shaking, the color reaction was read at 570 nm with a Titertek Multiskan

For the histological study, at each time of culture, the biomaterials were fixed in a 4% paraformaldehyde phosphate-buffered saline at 4 $^{\circ}\text{C}$, dehydrated in graded ethanol, defatted in propylene oxide and finally embedded in Epon B to allow semi-thin sections. Cells were stained with methylene blue. A part of the biomaterials was preserved for SEM observation [14, 15].

3. Results

3.1. Effect of porogen addition on the interconnection of macropores

In order to investigate the influence of the porogen size and content on interconnections, materials were processed with 600–1250 or 300–600 μm porogen particles (Fig. 1) and with porogen contents ranging from 0 to 60 vol % of the dry matter content (Fig. 2). After casting and debinding, ceramic materials were all sintered at 1125 $^{\circ}\text{C}$ for 15 h and the resulting interconnection size distribution and content were quantified by mercury intrusion porosimetry.

Two types of interconnections are observed on Fig. 1: interconnections between macroporosities and interconnections between microporosities. Their size ranges from 2 to 80 μm and 0.3 to 2 μm , respectively.

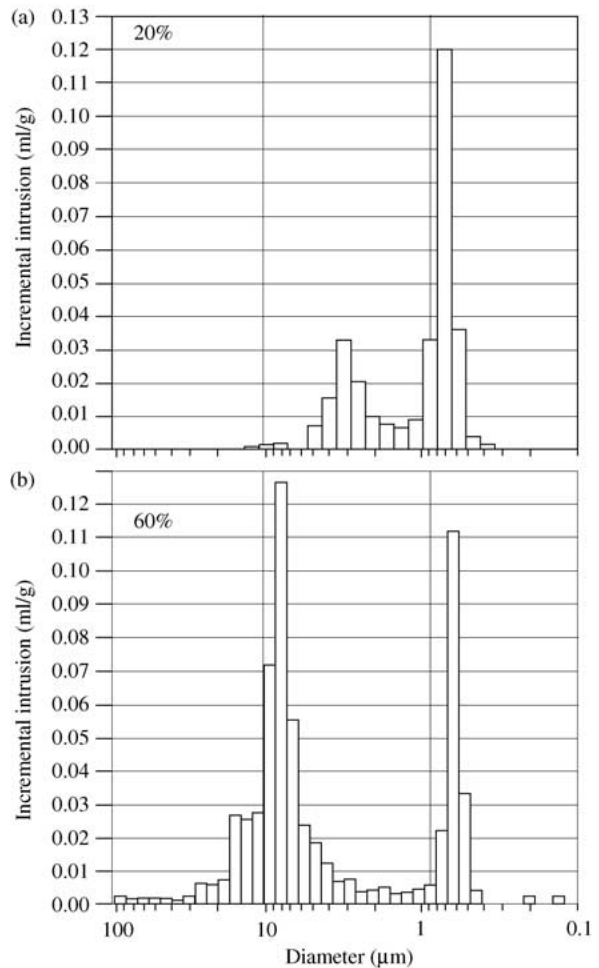


Figure 2 Mercury intrusion diagrams (mercury intrusion volume vs. interconnection diameter) for porogen volume ratios of 20% (a) and 60% (b). Sintering: 1125 $^{\circ}\text{C}$ during 15 h, porogen particles size: 600–1250 μm .

Microinterconnections are not influenced by the porogen size. In contrast, macrointerconnections are shifted from a mean size of about 30 μm , with 600–1250 μm porogen particles, to 15 μm , with 300–600 μm particles.

Fig. 2 shows the volume fraction of micro and macrointerconnections for two selected volume fractions (20% and 60%) of porogen (600–1250 μm). For 0% porogen, some macrointerconnections were already detected. They are produced by the strengthening polymer, which contributes to generate macrointerconnections. As expected, the macrointerconnection content increases with the porogen ratio because the number of contacts between porogen particles is increased when the porogen particles get nearer in the slurry. The size of macrointerconnections increases with the porogen ratio: for 20 vol % of porogen, medium macrointerconnection size is 3 μm whereas for 60 vol % it reaches 10 μm .

Macrointerconnectivity is thus effective in these materials. The content of macrointerconnections increases with the porogen ratio and their size increases with both the porogen ratio and size.

3.2. Effect of sintering temperature on micropores

Materials with 35 vol % of 600–1250 μm porogen particles were processed and sintered for 6 h at temperatures

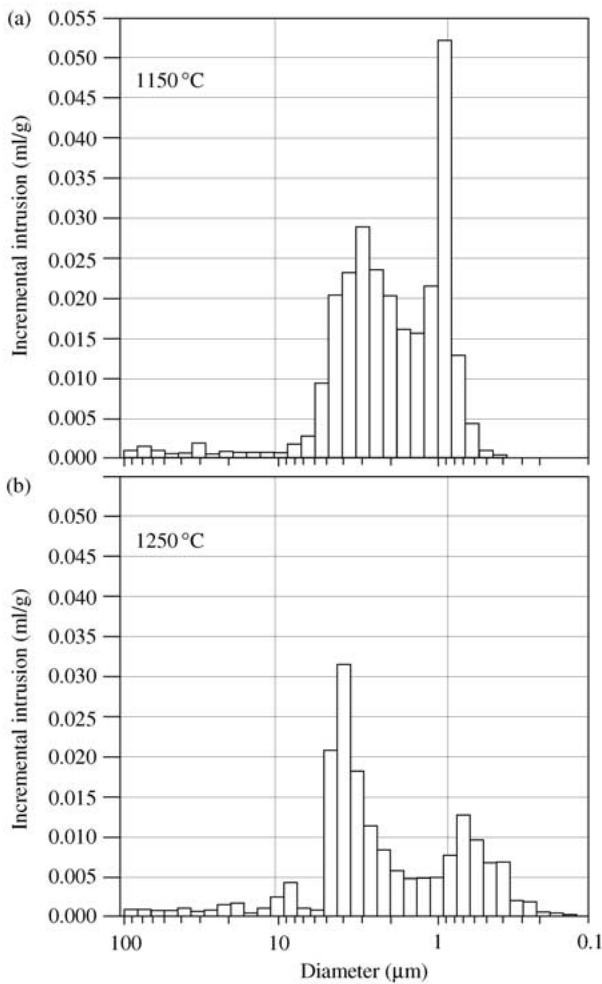


Figure 3 Mercury intrusion diagrams (mercury intrusion volume vs. interconnection diameter) for bone substitutes sintered during 6 h at temperatures of 1150 °C (a) and 1250 °C (b). Porogen content: 35 vol % of 600–1250 μm particles.

ranging from 1150 to 1250 °C. The volume fraction and size of interconnections were measured as a function of the sintering temperature (Fig. 3).

The size of microinterconnections is not influenced by

the sintering temperature but their content decreases. At the same time, macrointerconnection size slightly increases (from a mean size of 2.6 μm at 1150 °C to 3.7 μm at 1250 °C). This is in agreement with general sintering mechanisms: below a critical size (micropores), pores tend to disappear and above (macropores) their size increases [16].

3.3. Effect of porosity on compressive strength

Increasing porosity leads to a decrease of mechanical strength. Exponential functions are generally used to describe the strength–porosity dependence of ceramics [17]:

$$\sigma_R = \sigma_0 \cdot \exp(-b \cdot p) \quad (1)$$

σ_R being the strength for a volume fraction of pores p (%), σ_0 the strength of the material without pores and b a constant related to the sensitivity of the material to porosity. These functions are phenomenological by nature.

Here, two types of pores must be taken into account: micro- and macroporosities. Ceramics being sensitive to the most critical defect, this is the macroporosity which is of major importance. We may thus consider that σ_0 is the strength of the material without porogen addition (containing only micro- and macropores induced by the strengthening agent) and p is the porogen content (vol %). The influence of the porogen ratio on compressive strength was studied first (Fig. 4). 300–600 and 600–1250 μm porogen particles were introduced with ratio ranging from 0 to 65 vol %. All the materials were sintered at 1125 °C for 15 h.

In this experiment, σ_0 value is 37.5 MPa. The results obtained for the two porogen particle sizes can be well fitted by Equation 1 but with two different b parameters. The larger the porogen particles, the higher the b parameter value (2 and 4 for 300–600 and 600–1250 μm porogen size, respectively). This is in agree-

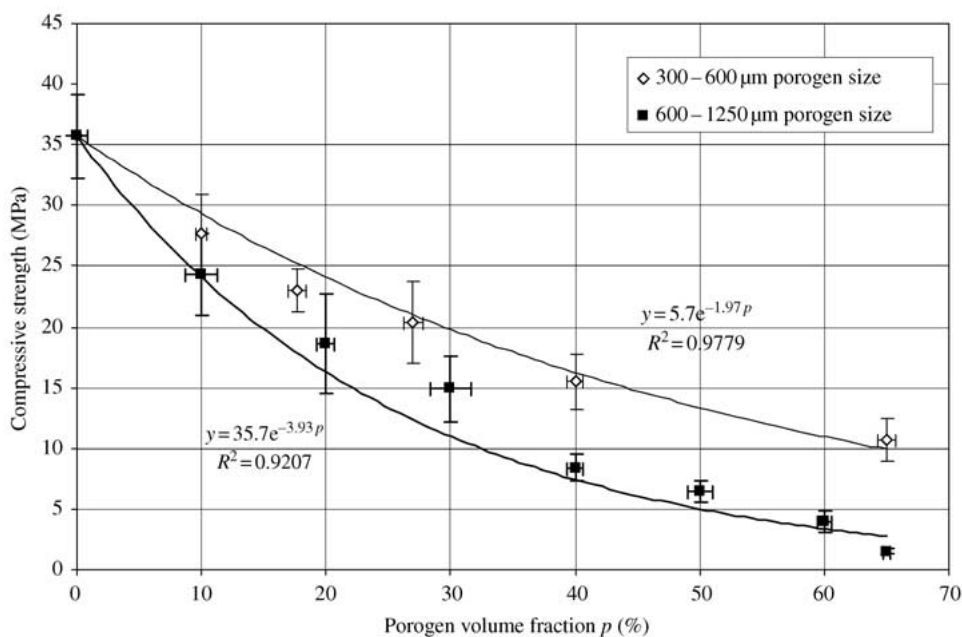


Figure 4 Compressive strength vs. porogen volume ratio for bone substitutes processed with 300–600 and 600–1250 μm porogen particles. Sintering: 1125 °C during 15 h.

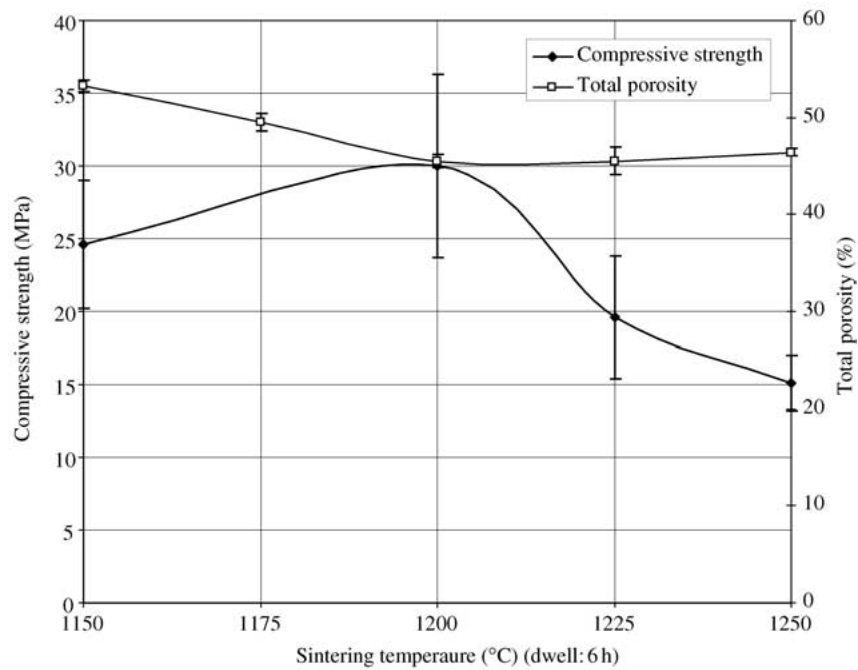


Figure 5 Compressive strength and total porosity of bone substitutes processed with 35 vol % of 600–1250 μm porogen particles and sintered for 6 h at different temperatures.

ment with the common idea that mechanical strength of brittle materials like ceramics is governed by the largest defect. In those materials the largest defects are the macropores; this explains that the strength of 600–1250 μm materials is very low.

In order to investigate the effect of the sintering temperature on mechanical strength, a series of materials was processed with the same amount (35 vol %) and size (600–1250 μm) of porogen particles, but sintered for 6 h at different temperatures (ranging from 1150 to 1250 $^{\circ}\text{C}$).

Fig. 5, total porosity decreases from 1150 to 1200 $^{\circ}\text{C}$, then stabilizes (a slight increase may even be observed from 1200 to 1250 $^{\circ}\text{C}$). It can be concluded that the sintering process is complete after 6 h at 1200 $^{\circ}\text{C}$. 1200 $^{\circ}\text{C}$ also corresponds to an acceleration of grain growth (Fig. 6). It is well known that the strength of ceramic materials is function of porosity and grain size.

The lower the porosity content, the higher the strength. On the other hand, the larger the grain size, the lower the strength. Thus, an optimum generally appears, which is here obtained for a sintering temperature of 1200 $^{\circ}\text{C}$ and corresponds to a grain size of 2.5 μm .

3.4. Choice and characterization of three materials for *in vitro* cell culture

The aim of this study was to compare materials with a large range of micro and macroporosity properties by cell culture tests *in vitro*. Using the previous results, three materials A, B, and C were processed and characterized. Materials A and B were processed with two different porogen particle size: 600–1250 and 300–600 μm , respectively, but with the same ratio of 65 vol %. This ratio was chosen in order to increase contacts between

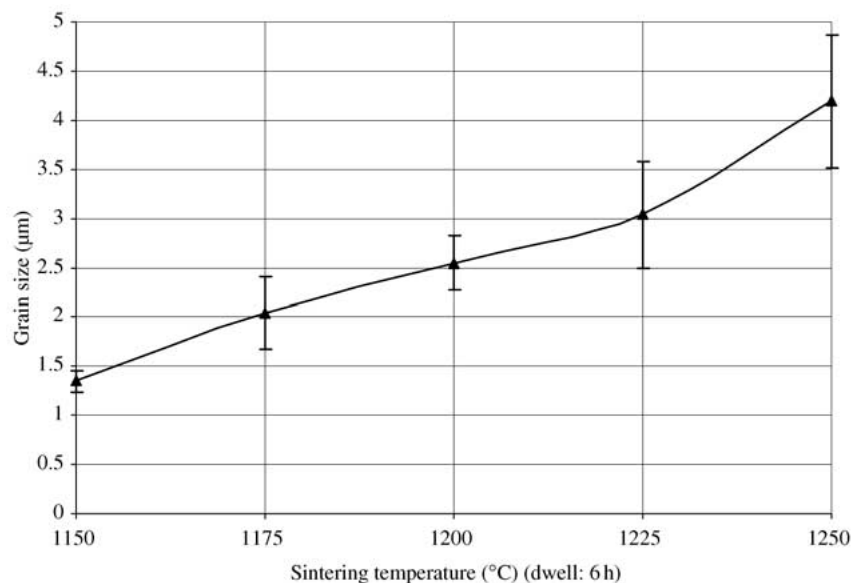


Figure 6 Grain size vs. temperature for bone substitutes processed with 35 vol % of 600–1250 μm porogen particles and sintered for 6 h.

TABLE I Physico-chemical characteristics of bone substitutes A, B, and C

Type of blocks	A	B	C
Macroporosity	600–1250 μm	300–600 μm	300–600 μm
Macrointerconnection size (mercury porosimetry)	30 μm	15 μm	15 μm
Sintering	1125 °C, 15 h	1125 °C, 15 h	1300 °C, 6 h
Grain size	1–2 μm	1–2 μm	18 μm
Microporosity content	18%	18%	2%
BET specific surface area	1.01 m^2/g	0.87 m^2/g	0.17 m^2/g
Total porosity	73.0 \pm 0.3%	68.7 \pm 0.7%	53 \pm 2%
Compressive strength	1.5 \pm 0.2 MPa	11 \pm 2 MPa	22 \pm 7 MPa

porogen particles in the slurry and thus macrointerconnections number (their mercury intrusion diagrams are given Fig. 1(a) and (b), respectively). A and B materials were both sintered at low temperature (1125 °C) in order to keep a high volume ratio of microporosity and small grains. A long sintering dwell (15 h) was thus necessary to allow densification. Materials B and C were both processed with 65 vol % of 300–600 μm porogen particles but material C was voluntarily sintered at high temperature (1300 °C during 6 h) in order to obtain a low microporosity ratio and large grains. All the biomaterials

were then washed in alcohol and sterilized by gamma irradiation. The respective properties of the biomaterials were measured and are given in Table I.

Differences in porogen size between materials A and B (Fig. 7(a) and (b)) generate differences in macrointerconnection size. They also lead to a large difference in compressive strength. Other microstructural parameters are roughly the same for materials A and B. Materials B and C differ by their sintering temperature. This leads essentially to a change in microporosity content (Fig. 7(c) and (d)) and grain size. BET specific

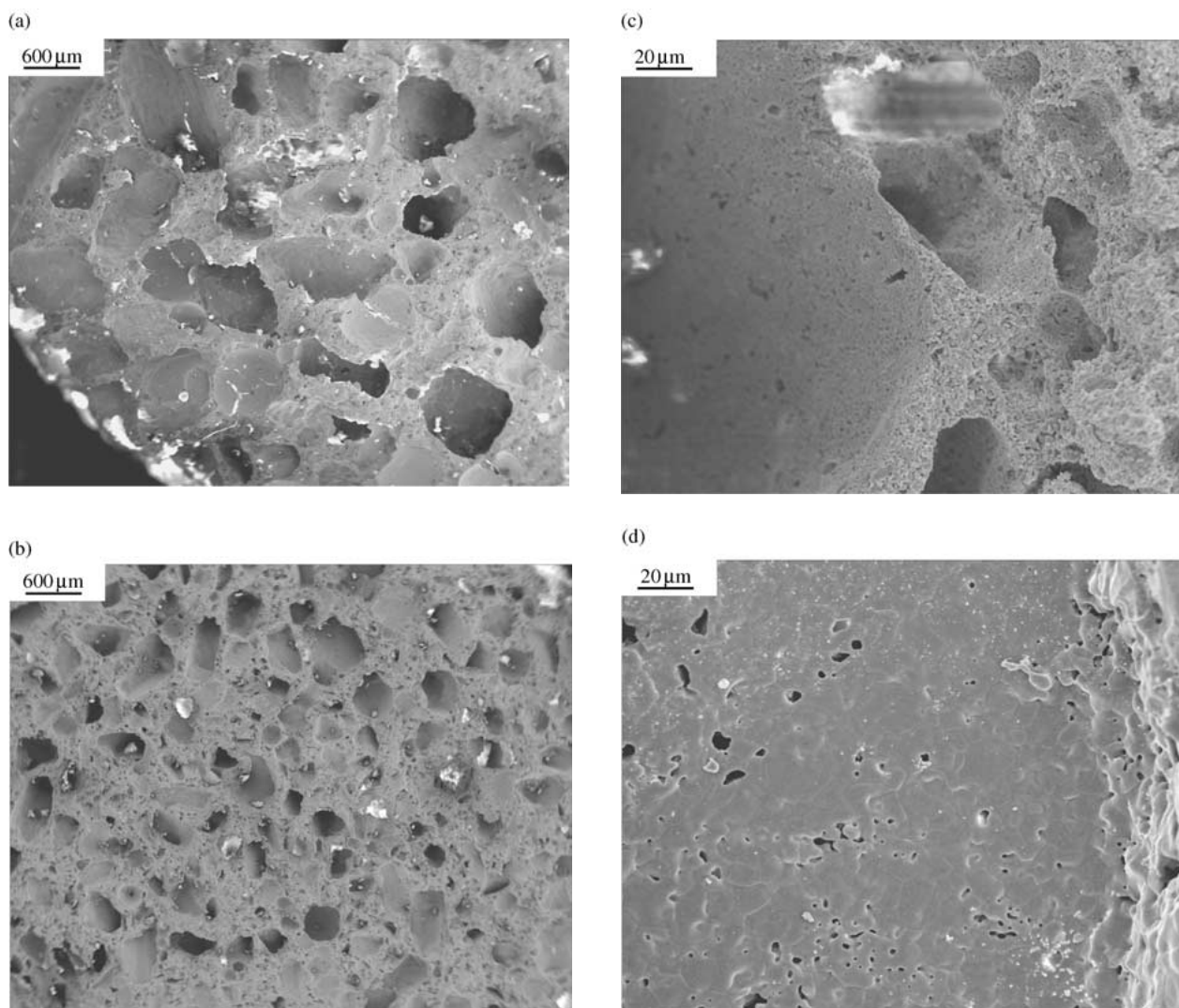


Figure 7 SEM observations of bone substitutes. (a) macroporosity in material A; (b) macroporosity in material B (i.e. material C), (c) microporosity in material B (i.e. material A), (d) microporosity in material C.

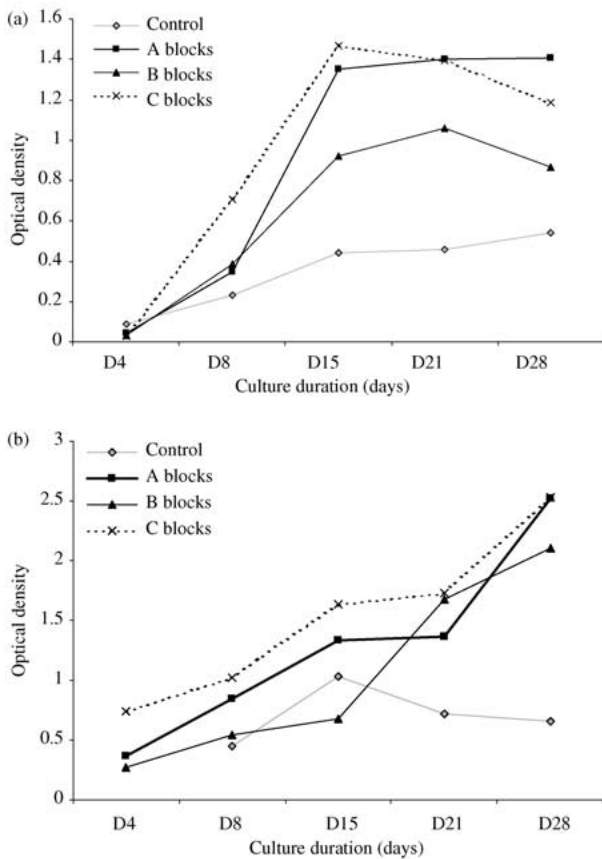


Figure 8 Results of MTT tests on osteoblast cultures (a) and fibroblast cultures (b).

surface area was measured for each series of materials. As expected, its value decreases for high sintering temperature (material C compared to material B) while it is not significantly influenced by the porogen size (A and B materials).

3.5. *In vitro* characterization of the materials by cell culture

Cellular viability (evaluated by MTT test) is satisfactory on the three materials (Fig. 8) [14, 15]. No cytotoxicity is observed, as an exponential cellular growth is effective on every material for both osteoblasts and fibroblasts. The proliferation of fibroblasts being higher than those of osteoblasts, their cellular density is higher, whatever the material. For osteoblasts, a decrease of MTT curves is observed after day 21 and day 15 for B and C materials, respectively, due to contact inhibition (Fig. 8(a)). For A material, no contact inhibition is observed. With fibroblasts, which are smaller than osteoblasts, no contact inhibition occurred with any of the three materials (Fig. 8(b)).

Fig. 9 presents histological observations of osteoblasts on material B. The cellular density is higher on the surface of the material than in the depth. Cells cover the whole surface of the material, bridging macroporosity. Cellular growth is also observed in the macroporosity, leading to the invasion of the depth of the material. Those first observations were the same for A and C materials.

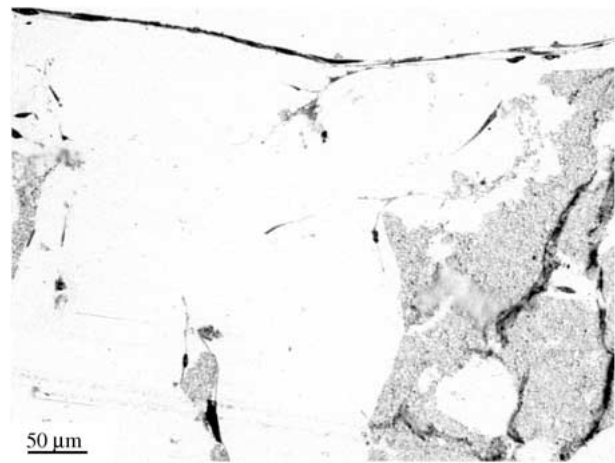


Figure 9 Histological observation of bone substitute B after 21 days of osteoblast culture: cells bridging the macroporosity and invading the porous volume.

Osteoblasts and fibroblasts colonized 1.6 mm depth of the material A and 1 mm depth of the materials B and C. Interconnections of 15 μm size are thus efficient to allow the migration of cells between macropores.

With SEM observations, a better understanding of cell invasion mechanisms is possible. During the first days, cellular growth is centrifugal from the initial drop of culture serum loaded with cells. Observations conducted at day 21 show that the surface of the materials is completely covered by cells (Fig. 10). Bridging of macroporosity is possible because of the emission by the cells of cytoplasmic extensions across macropores (Fig. 11). At the same time, the invasion of the macroporosity is observed with cells spreading on macropores surface and invading the porous volume (Fig. 12). A lot of cell attachments on microporosity were observed with materials A and B (Fig. 13). Cytoplasmic extensions spread on microporosity and penetrate inside. Fewer cell attachments were observed on dense macropores surface of material C, which tends to demonstrate the affinity of cells for microporosity.

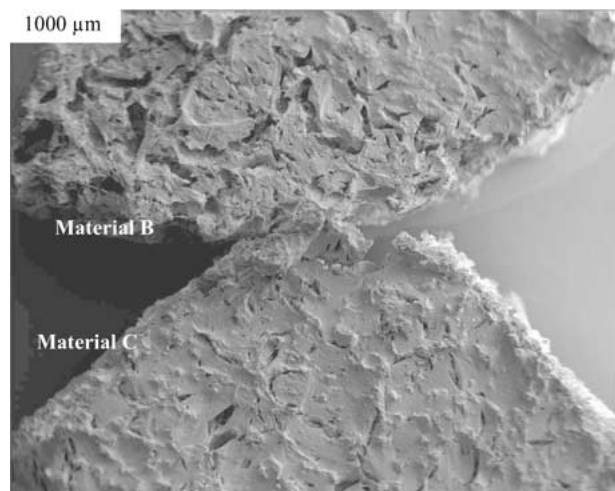


Figure 10 SEM observation of the surface of bone substitutes B and C after 21 days of osteoblast culture: the surface is completely covered by cells.

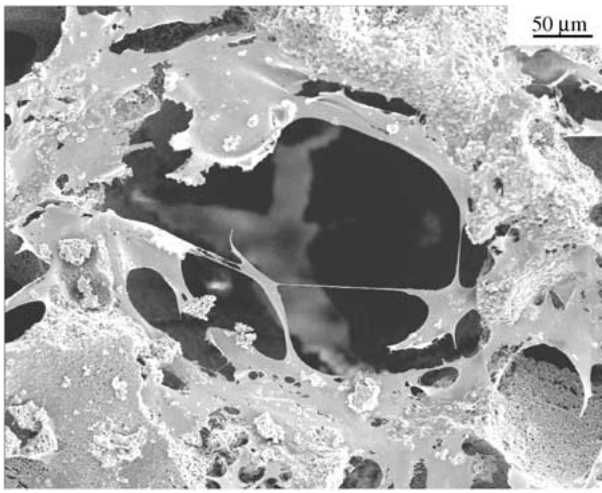


Figure 11 SEM observation of the surface of bone substitute B after 8 days of osteoblast culture: bridging of a macropore by the emission of cytoplasmic cell extensions.

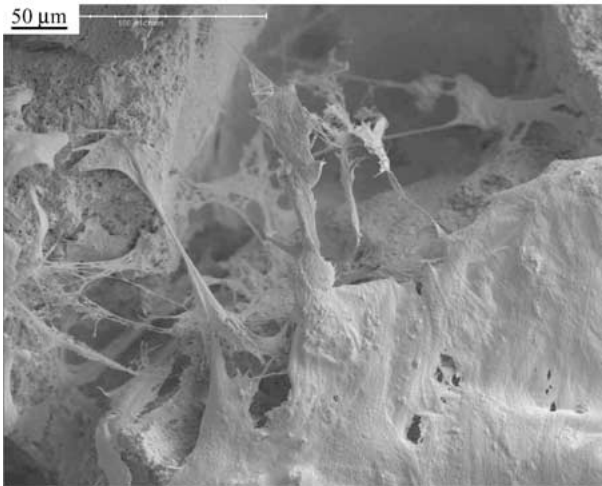


Figure 12 SEM observation of bone substitute B after 21 days of osteoblast culture. Foreground: osteoblasts covering the surface. Background: cell penetrating into the macroporosity and colonising the porous volume.

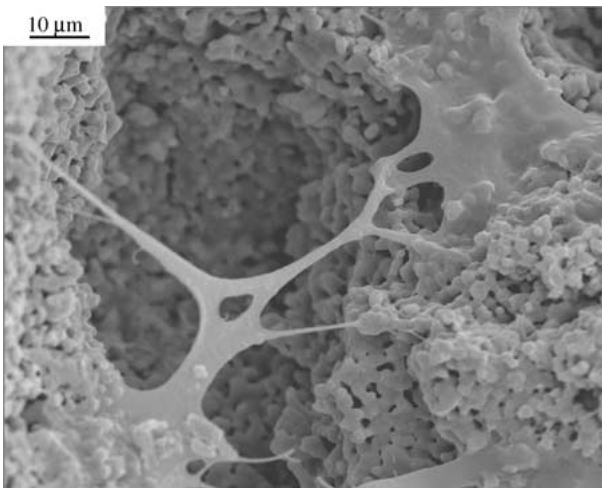


Figure 13 SEM observation of an osteoblast hanging on microporosity of bone substitute B after 8 days of culture.

4. General discussion

Four main key points can be discussed:

1. None of the three materials appears as cytotoxic. It is well known that calcium phosphate ceramics are biocompatible but studies had put forward that hydroxyapatite fine particles (i.e. with high specific area) could be cytotoxic because of cell membrane damages [18]. This was not observed in this study and no difference was observed between materials B ($0.87 \text{ m}^2/\text{g}$) and C ($0.17 \text{ m}^2/\text{g}$). Thus, rather than specific surface area, the cytotoxicity should be attributed to the morphology of ceramic grains, i.e. their shape and size. The round shaped grains of the three materials seem to be suitable for cell activity.

2. The emission by the cells of cytoplasmic extensions and their hanging on microporosity appear to be of main importance for cell spreading. The attachment of extensions on microporosity tends to favor both cell intrusion in the material and the bridging of macropores. However, microporosity is not completely necessary, as cell ingrowth is also effective with material C, with a low microporosity content. Further studies should focus on this point. It is to note that microporosity increases material resorption *in vivo* [6, 19]. Furthermore, its influence on material mechanical strength is lower than the influence of macroporosity. It seems thus better to increase its ratio for bone substitutes.

3. Former studies demonstrated that bone ingrowth was favored by large macroporosity content [20]. However, the different investigations found in the bibliography are difficult to compare in order to define an optimal macroporosity size. Other material parameters can vary (in particular macrointerconnections, which are of large importance but are generally not quantified). Here, the characterization of other parameters was conducted as exhaustively as possible. Colonization of the depth of material A with 600–1250 μm macroporosity appears to be easier than the colonization of materials B and C with 300–600 μm porosity. Those results can be explained by the simple hypothesis that the difficulty for cells is not to colonize a macropore but to pass through interconnections. Thus, with larger macropores, fewer interconnections have to be passed through by the cells, and the colonization rate is high. More than the size of the macropores, the density of interconnections rules the colonization rate. Macrointerconnection size is also of key importance. For Lu *et al.* [5], the macrointerconnection size must be larger than 20 μm to allow cell ingrowth. In this study the biomaterials have macrointerconnection size ranging from 15 to 30 μm . This size appears to be efficient for cell ingrowth. For Liu [6], bone ingrowth/formation is also possible within porous implants having pores in the order of a few microns or less. However, as cells and body fluids have to pass through macrointerconnections, the larger their size, the easier the cell ingrowth.

4. Large and numerous macrointerconnections mean low strength. Thus, none of the materials A, B, and C processed should be suitable for mechanical bearing applications. The influence of the macroporosity size on mechanical strength is very strong and compressive strength of material A is low. Such a material can only be

used for surgery when appropriate complementary apparatus fulfils the mechanical function. For example, material A should be appropriate to fill in an arthrodesis metal or polymer cage. Material C is the strongest material processed, because of its low microporosity content, but it can be guessed that its resorbability rate will be slower than for material B. Moreover microporosity of material B seems to favor cell hanging on the material. For most applications, a compromise has to be found between mechanical strength and osteoconduction potential. Material B with a medium macrointerconnection size of 15 μm is efficient to allow cell ingrowth and to bear a compressive strength of 10 MPa.

5. Conclusion

The morphology of porosity influences cell spreading and cell ingrowth in bone substitutes. Macrointerconnections are necessary to promote cell ingrowth and microporosity seems to influence cell hanging on the material. However, porosity has a detrimental influence on mechanical strength, which directly influences the device handiness when surgeons have to machine the blocks. It is generally admitted that mechanical strength is not an important parameter for bone substitutes, but a material with low mechanical properties will crumble under cyclic stresses and the resulting micromovements should generate fibrous tissue encapsulation. Mechanical strength, macrointerconnections and surface physico-chemical characteristics of bone substitutes are thus of equal importance and none must be neglected to guarantee clinical success. As it is generally difficult to find a compromise, it is better to tailor the material porosity to fit the functionality required.

In a prospective point of view, bone tissue engineering is today considered as a promising approach for second generation bone substitutes. HAP:TCP porous materials are suitable scaffolds for osteoblast cell cultures. A full understanding of cell attachment and spreading mechanisms on these scaffolds will be necessary to develop hybrid bones. In particular, the influence of parameters like microporosity will have to be studied.

Acknowledgments

This work was supported by Coating Industries (69621 Vaulx-En-Velin, France) who provided the core funding and the hydroxyapatite powder used in this study. The authors express their gratitude to A.C. Maurin and D. Farlay for their expert technical assistance.

References

1. R. CAVAGNA, G. DACULSI and J.-M. BOULER, *J. Long-Term Effects Med. Implants* **9** (1997) 403.
2. T. KOSHIMO, T. MURASE, T. TAKAGI and T. SAITO, *Biomaterials* **22** (2001) 1579.
3. P. DUCHEYNE, S. RADIN and L. KING, *J. Biomed. Mater. Res.* **27** (1993) 25.
4. G. DACULSI, R. Z. LEGEROS, E. NERY, K. LYNCH and B. KEREBEL, *ibid.* **23** (1989) 883.
5. J. X. LU, B. FLAUTRE, K. ANSELME, P. HARDOUIN, A. GALLUR, M. DESCAMPS and B. THIERRY, *J. Mater. Sci., Mater. Med.* **10** (1999) 111.
6. D.-M. LIU, *Mater. Sci. Forum* **250** (1997) 183.
7. M. AKAO, N. MIURA and H. AOKI, *Yogyo-Kyokai-Shi* **92** (1984) 672.
8. T. HUSSAIN, A. GHOLINIA and C. LEACH, *Key Eng. Mater.* **132** (1997) 544.
9. C. BENAQQA, J. CHEVALIER, M. SAËDAOUI and G. FANTOZZI, *ibid.* **206** (2002) 1641.
10. H. YUAN, K. KURASHINA, J. D. BRUIJN, Y. LI, K. DE GROOT and X. ZHANG, *Biomaterials* **20** (1999) 1799.
11. A. BIGNON, J. CHEVALIER and G. FANTOZZI, *J. Biomed. Mater. Res. App. Biomat.* **63** (2002) 619.
12. M. I. MENDELSON, *J. Am. Ceram. Soc.* **52** (1969) 443.
13. T. MOSMANN, *Cell. Immunol.* **65** (1983) 55.
14. J. CHOUTEAU, *Mémoire de DEA, Faculté de médecine, Lyon* (2001) p. 72.
15. J. CHOUTEAU, A. BIGNON, P. CHAVASSIEUX *et al.*, *Rev. Chir. Orthop. Répar. Mot.* (in French) **89** (2003) 44.
16. D. BERNACHE-ASSOLLANT, *L'industrie céramique & verrière* **925** (1997) 257.
17. D.-M. LIU, *Ceram. Int.* **23** (1997) 135.
18. J.-S. SUN, H.-C. LIU and W.H.-S. CHANG *et al.*, *J. Biomed. Mater. Res.* **39** (1998) 390.
19. N. PASSUTI, J. DELECRIN, F. GOUIN and D. HEYMANN, in "Substituts osseux" *Encycl. Méd. Chir.* 14-015-B-10 (Elsevier, Paris, 1999) p. 1.
20. O. GAUTIER, J. M. BOULER, E. AGUADO, P. PILET and G. DACULSI, *Biomaterials* **19** (1998) 133.

Received 7 May 2002

and accepted 14 April 2003